Duration and nature of the end-Cryogenian (Marinoan) glaciation

[1]Anthony R. Prave, [2]Daniel J. Condon, [3]Karl Heinz Hoffmann, [2]Simon Tapster, and [4]Anthony E. Fallick

[1]Department of Earth and Environmental Sciences, University of St Andrews, St Andrews, KY16 9AL, UK

[2]NERC Isotope Geosciences Laboratory, British Geological Survey, Nottingham, NG12 5GG, UK

[3]Geological Survey of Namibia, 1 Aviation Road, Windhoek, Namibia

[4]Scottish Universities Environmental Research Centre, East Kilbride, G75 0QF, UK

ABSTRACT

The end-Cryogenian glaciation (Marinoan) was Earth's last global glaciation yet its duration and character remain uncertain. Here we report U-Pb zircon ages for two discrete ash beds within glacimarine deposits from widely separated localities of the Marinoan-equivalent Ghaub Formation in Namibia: 639.29 ± 0.26/0.31/0.75 Ma and 635.21 ± 0.59/0.61/0.92 Ma. These findings, for the first time, verify the key prediction of the Snowball Earth hypothesis for the Marinoan glaciation: longevity, with a duration of ≥4.08 ± 0.64 Myr. They also show that glacigenic sedimentation, erosion, and at least intermittent open-water conditions occurred 4 million years prior to termination of the Marinoan glaciation and that the interval of non-glacial conditions between the two Cryogenian glaciations was 20 Myr or less.

INTRODUCTION

The Cryogenian Period (*c*. 720 – 635 Ma) was marked by the two most severe glaciations in Earth history (Hoffman et al., 1998; Fairchild and Kennedy, 2007), the older Sturtian and younger Marinoan, and their association with unique lithofacies of cap carbonates (Kennedy et al., 2001; Hoffman and Schrag, 2002; Hoffman et al., 2011), stable isotope fluctuations (carbon, oxygen, boron, calcium; Halverson et al., 2005; Kasemann et al., 2005; Bao et al., 2008) and banded iron formation are evidence for global-scale environmental changes with postulated links to ocean-

atmosphere oxygenation and biosphere evolution (Butterfield, 2009; Och and Sjields-Zhou, 2012; Sperling et al., 2013). Creation of a unified theory explaining those phenomena, however, has been hampered by one key obstacle: a lack of temporal constraints. Recently, the Sturtian was shown to have spanned an astonishing 56 Myr, from about 716 Ma to 660 Ma (Bowring et al., 2007; Macdonald et al., 2010; Rooney et al., 2014; Rooney et al., 2015). In contrast, the duration of the Marinoan is unresolved: it terminated at *c*. 635 Ma (Hoffmann et al. 2004; Calver et al., 2004; Condon et al., 2005; Zhang et al., 2008) but its initiation can only be stated as being younger than interglacial strata, which in Mongolia have been dated as *c*. 659 Ma (Rooney et al., 2014) and in China as *c*. 655 Ma (Zhang et al., 2008). Here we report new dates for the Marinoan-equivalent Ghaub Formation in Namibia that provide a basis for assessing the timing and nature of Earth's last global glaciation.

GEOLOGY: SAMPLES DW-1 AND NAV-00-2B

The Nosib, Otavi and Mulden Groups comprise the Neoproterozoic sedimentary record of the Congo craton in northern Namibia (Fig. 1). The Otavi Group (and correlative rocks in the Swakop Group of the Outjo and Swakop Zones) is a 2-5 km thick carbonate platform-slope-basin succession formed in the tropics along the margin of the Congo Craton. It is punctuated by two Cryogenian glacial units (Hoffmann and Prave, 1996; Hofman and Halverson, 2008), the older Chuos and the younger Ghaub formations and their respective cap carbonates, the Rasthof and Keilberg formations. U-Pb zircon ages on igneous and volcanic units provide geochronological constraints (see Fig. 1) that bracket deposition of the glacigenic-bearing strata in the Otavi Group to between *c*. 756 Ma and 635 Ma.

One of the most informative exposures of the Ghaub Formation in northern Namibia is along Fransfontein Ridge (Fig. 1). There, the Ghaub rocks vary in thickness from 1 to 600 m and can be traced continuously for *c*. 70 km; they consist mostly of stratified and massive carbonate-clast-rich diamictite, minor intervals of rippled and cross-stratified dolomitic grainstone, marl and shale, and an upper unit, the 1 to 15 m thick Bethanis member (Hoffman and Halverson, 2008)

typified by cm- to dcm-thick stratified diamictite and grainstone-mudstone, all with abundant variably sized dropstones. Detailed studies (Hoffman and Halverson, 2008; Domack and Hoffmann, 2011) of those lithofacies have interpreted them as a succession of moraine and glacimarine sediments deposited along the margin of a repeatedly advancing and back-stepping ice-grounding line (Domack and Hoffmann, 2011).

Along Fransfontein Ridge, the diamictite-dominated Ghaub Formation contains lenses, generally a few metres thick, consisting of graded grainstone and laminated to massive calcareous-dolomitic marl-shale with stringers of dropstones. At Duurwater (Fig. 2) one of these lenses about 15 m below the base of the Keilberg cap dolostone contains a prominent ash bed, sampled as DW-1 (Fig. 3). The DW-1 ash bed is 0.3 m thick, pale tan to pale yellow in colour, characterised by sharp upper and lower contacts, displays a slight fining-upward grading, contains rare disseminated quartz spar crystals and is overlain and underlain by IRD beds (Fig. 4A). These features indicate that this bed is an air-fall tuff contemporaneous with deposition of the glacimarine sediments, hence its age would also be the age of sedimentation for this part of the Ghaub Formation. Below the DW-1 ash bed is 10-15m of massive diamictite and then a more than 100-m-thick succession of carbonate rhythmite, breccia, laminated marl and shale with dispersed dropstones and isolated metre-scale and larger blocks derived from pre-Ghaub formation units. These lithofacies fill a steep-sided incision cut into the pre-Ghaub stratigraphy (Figs. 2, 3); in places along the Fransfontein outcrop belt as much as 300 m of strata have been cut out along this surface.

Sample NAV-00-2B comes from an ash bed in the basinal equivalent of the Ghaub Formation *c*. 30 m below the contact with the Keilberg cap dolostone at Navachab in central Namibia (Fig. 3). This occurrence was reported by Hoffman et al. (2004) and readers are referred to that paper for details.

METHODS AND RESULTS

All zircon dates in this study were obtained using established chemical abrasion (CA) isotope dilution thermal ionisation mass spectrometry (ID-TIMS) methods at the NERC Isotope

79 Geoscience Laboratory of the British Geological Survey (Noble et al., 2015; see Data Repository
80 for details). U-Pb dates have been determined relative to the gravimetrically calibrated
81 EARTHTIME mixed U/Pb tracers (Condon et al., 2015; McLean et al., 2015) and ^{238}U and ^{235}U
82 decay constants (Jaffey et al., 1971; Mattinson, 2010).

83 Sample DW-1 yielded a population of zircons with a consistent morphology (aspect ratio ~2
84 and long axis typically 200 to 300 μm) and colour. Ten zircons were dated by CA-ID-TIMS; U-Pb
85 data for each analysis are concordant when the uncertainty in the ^{238}U and ^{235}U decay constants
86 (Mattinson, 2010) are considered (Fig. 4B; Data Repository Table 1). All analyses yield a weighted-
87 mean $^{207}Pb/^{206}Pb$ date of 639.1 ± 1.7/1.8/5.0 (n=10, MSWD=1.08). Of those, one analysis has
88 dispersion beyond that expected due to analytical scatter (see Data Repository) and is an obvious
89 outlier with a U-Pb date younger than the main population. Excepting this grain, the other nine
90 analyses yield a weighted mean $^{206}Pb/^{238}U$ date of 639.29 ± 0.26/0.31/0.75 Ma (95% confidence
91 interval, n=9, MSWD=2.6), which we interpret as the age of deposition.

92 Sample NAV-00-2B is an aliquot of the sample dated previously as 635.5 ±1.2 Ma
93 (Hoffmann et al., 2004) at the Massachusetts Institute of Technology. Re-analysis of this sample
94 was done to capitalise on the use of CA for the effective elimination of Pb-loss (Mattinson, 2005)
95 and the EARTHTIME tracer and its comprehensive gravimetric calibration and uncertainty model
96 (Condon et al., 2015; McLean et al., 2015). The $^{206}Pb/^{238}U$ date for NAV-00-2B derived in this
97 study is 635.21 ± 0.59/0.61/0.92 Ma (95% confidence interval, n=5, MSWD=3.4; Fig. 4B, Data
98 Repository Table 2). This date is based upon a subset of the analyses (as explained in the Data
99 Repository) and, even given improved analytical precision and accuracy, is indistinguishable from
100 the date published in Hoffmann et al. (2004).

101 **DISCUSSION**

102 The 639.29 ± 0.26/0.31/0.75 Ma age for the DW-1 ash bed at Duurwater and the revised age
103 of 635.21 ± 0.59/0.61/0.92 Ma for the NAV-00-2B ash bed at Navachab now, for the first time,
104 confirm that the Marinoan glaciation was long-lived, lasting at least 4.08 ± 0.64 Myr. This verifies

105 the key prediction of the Snowball Earth hypothesis for a long duration glaciation. The revised age
106 for NAV-00-2B also refines and reconfirms that the timing of termination of the Marinoan
107 glaciation was synchronous worldwide (*i.e*. within error of the age data), occurring between 635.21
108 ± 0.59/0.61/0.92 Ma and 635.2 ± 0.5 Ma, the age of an ash bed in the lower part of the cap
109 carbonate sequence in China (Condon et al., 2005); a conclusion reinforced by the U-Pb zircon age
110 of 636.41 ± 0.45 Ma for a volcaniclastic unit in the glacial-cap carbonate transition in Tasmania
111 (Calver et al., 2004).
112 Since the debut of the Snowball Earth hypothesis, debate has ensued regarding the extent of
113 land and sea ice during Cryogenian glaciations, the causes of repetitive patterns of inferred
114 proximal-distal and advance-retreat deposits, and the overall timing and duration of glacial
115 sedimentation (*e.g*. see discussion by Spence et al., 2016, and references therein). Further, the lack
116 of well-defined age models has led to an array of climate state and sedimentation scenarios, ranging
117 from surmising that the Marinoan rock record formed by glacial-interglacial-scale epochs (*e.g*.
118 Allen and Etienne, 2008; LeHeron et al., 2011) to interpretations of the bulk of that record as
119 having been deposited during a brief interval of time near to the end of the glacial state (*e.g*. Benn et
120 al., 2015). Although these interpretations are not necessarily mutually exclusive, assessing them
121 remains speculative because of the lack of constraints for the absolute timing of sedimentation. Our
122 new geochronological data provide a better temporal framework for understanding the Marinoan
123 glaciation. For example, the *c*. 639 Ma DW-1 ash bed occurring above a *c*. 100-m-thick glacimarine
124 succession shows that glacial erosion and sediment accumulation concurrent with at least
125 intermittent open-water conditions in the tropics existed more than 4 million years before the
126 ultimate meltback phase of the Marinoan ice sheets. This impacts on a range of issues regarding the
127 Marinoan climate state: it provides constraints and corroboration of models that yield results
128 consistent with such conditions, including predictions of plausible CO_2 levels permissive of
129 enabling ice-line migration and associated sedimentation in the tropics, as documented for the
130 Ghaub Formation (e.g. Domack and Hoffman, 2011), to considerations of low-latitude *refugia* and

the survival of eukaryotic organisms within the main phase of the Marinoan glaciation. Further, given our new age that provides a minimum duration for the Marinoan glaciation and the *c*. 660 Ma age for the end of the older Cryogenian glaciation (Sturtian), the intervening interglacial interval and associated biogeochemical and isotopic events represent a timespan of 20 Myr or less (Fig. 4C). Determining how and why this period of non-glacial conditions punctuated an otherwise apparently consistently and largely ice-covered Earth poses an intriguing research question.

CONCLUSION

The 639.1 ± 1.7/1.8/5.0 Ma age obtained on an ash bed in glacimarine sediments of the Marinoan-equivalent Ghaub Formation in northern Namibia combined with a refined age of 635.21 ± 0.59/0.61/0.92 Ma for an ash bed in the basinal equivalent of the Ghaub Formation in central Namibia confirm that the Marinoan glaciation was long-lived, at least 4 Myr in duration, and that the preceding interval of non-glacial conditions was less than 20 Myr in duration. Our data also confirm that the sedimentary archive of the Marinoan glaciation records glacial erosion-sedimentation and at least intermittent open-water conditions as much as 4 million years prior to terminal meltback at *c*. 635 Ma.

ACKNOWLEDGMENTS

This work was supported by NIGFSC grant IP XXXXX.

REFERENCES CITED

Allen, P.A., and Etienne, J.L., 2008, Sedimentary challenge to Snowball Earth: Nature Geosciences, v. 1, p. 817-825.

Bao, H., Lyons, J.R., and Zhou, C., 2008, Triple oxygen isotope evidence for elevated CO2 levels after a Neoproterozoic glaciation: Nature, v. 453, p. 504-506.

156 Benn, D.I., Le Hir, G., Bai, H., Donnadieu, Y., Dumas, C., Fleming, E.J., Hambrey, M.J.,
157 McMillan, E.A., Petronis, M.S., Ramstein, G, Stevenson, C.T.E., Wynn, P.M., Fairchild, I.J.,
158 2015, Orbitally forced ice sheet fluctuations during the Marinoan Snowball Earth glaciation:
159 Nature Geoscience, v. 8, p. 704-707.
160 Bowring, S.A., Grotzinger, J.P., Condon, J., Ramezani, J., Newall, M.J., and Allen, P.A., 2007,
161 Geochronologic constraints of the chronostratigraphic framework of the Neoproterozoic Huqf
162 Supergroup, Sultanate of Oman: American Journal of Science, v. 307, p. 1097-1145.
163 Butterfield, N.J., 2009, Oxygen, animals and oceanic ventilation: an alternative view: Geobiology,
164 v. 7, p. 1-7.
165 Calver, C.R., Black, L.P., Everard, J.L., and Seymour, D.B., 2004, U-Pb zircon age constraints on
166 late Neoproterozoic glaciation in Tasmania: Geology, v. 32, p. 893-896.
167 Condon, D.J., Schoene, B., McLean, N.M., Bowring, S.A., and Parrish, R.R., 2015, Metrology and
168 traceability of U-Pb isotope dilution geochronology (EARTHTIME Tracer Calibration Part I):
169 Geochimica et Cosmochimica Acta, v. 164, p. 464-480,
170 Condon, D., Zhu, M., Bowring, S., Wang, W., Yang, A., and Jin, Y., 2005, U-Pb ages from the
171 Neoproterozoic Doushantuo formation, China: Science, v. 308, p. 95-98.
172 Cox, G.M., Strauss, J.V., Halverson, G.P., Schmitz, M.D., McClelland, W.C., Stevenson, R.S., and
173 Macdonald, F.A., 2015, Kikiktat volcanics of Arctic Alaska – melting of harzburgitic mantle
174 associated with the Franklin large igneous province: Lithosphere L435-1. DOI:
175 10.1130/L435.1.
176 Domack, E.W., and Hoffman, P.F., 2011, An ice grounding-line wedge from the Ghaub glaciation
177 (635 Ma) on the distal foreslope of the Otavi carbonate platform, Namibia, and its bearing on
178 the snowball Earth hypothesis: Geological Society of America Bulletin, v. 123, p. 1448-1477.
179 Fairchild, I.J., and Kennedy, M.J., 2007, Neoproterozoic glaciation in the Earth System: Journal of
180 the Geological Society, v. 164, p. 895-921.

Halverson, G.P., Hoffman, P.F., Schrag, D.P., Maloof, A.C., and Rice, A.H.N., 2005, Toward a Neoproterozoic composite carbon-isotope record: Geological Society of America Bulletin, v. 117, p. 1181-1207.

Hoffman, P.F., 2011, Strange bedfellows: glacial diamictite and cap carbonate from the Marinoan (635 Ma) glaciation in Namibia: Sedimentology, v. 58, p. 57-119.

Hoffman, P.F., and Halverson, G.P., 2008, Otavi Group of the western Northern Platform, the eastern Kaoko Zone and the Northern Margin Zone, *in* Miller, R.McG., ed., The Geology of Namibia: Volume 2 Neoproterozoic to Lower Palaeozoic: Ministry of Mines and Energy, Namibia, p. 13-69–13-136.

Hoffman, P.F., Hawkins, D.P., Isachsen, C.E., and Bowring, S.A., 1996, Precise U-Pb zircon ages for early Damaran magmatism in the Summas Mountains and Weltwischia Inlier, northern Damara Belt, Namibia. Communications of the Geological Survey of Namibia 11, 47-52.

Hoffman, P.F., Kaufman, A.J., Halverson, G.P., and Schrag, D.P., 1998, A Neoproterozoic snowball Earth: Science, v. 281, p. 1342-1346.

Hoffman, P.F., and Schrag, D.P., 2002, The snowball Earth hypothesis: testing the limits of global change: Terra Nova, v. 14, p. 129-155.

Hoffmann, K.H., Condon, D., Bowring, S., and Crowley, J., 2004, U-Pb zircon date from the Neoproterozoic Ghaub Formation, Namibia: constraints on Marinoan glaciation: Geology, v. 32, p. 817-821.

Hoffmann, K.H., and Prave, A.R., 1996, A preliminary note on a revised subdivision and regional correlation of the Otavi Group based on glacigenic diamictites and associated cap dolostones: Communications of the Geological Survey of Namibia, v. 11, p. 77-82.

Jaffey, A.H., Flynn, K.F., Glendenin, L.E., Bentley, W.C., and Essling, A.M., 1971, Precision measurement of half-lives and specific of ^{235}U and ^{238}U: Physics Reviews C4, p. 1889-1906.

Kasemann, S.A., Hawkesworth, C.J., Prave, A.R., Fallick, A.E., and Pearson, P.N., 2005, Boron and calcium isotope composition in Neoproterozoic carbonate rocks from Namibia: evidence for extreme environmental change: Earth and Planetary Science Letters, v. 231, p. 73-86.

Kennedy, M.J., Christie-Blick, N., and Prave, A.R., 2001, Carbon isotopic composition of Neoproterozoic glacial carbonates as a test of paleoceanographic models for snowball Earth phenomena: Geology, v. 29, p. 1135-1138.

Le Heron, D.P, Cox, G., Trundley, A., and Collins, A.S., 2011, Two Cryogenian glacial successions compared: Aspects of the Sturt and Elatina sediment records of South Australia: Precambrian Research, v. 186, p. 147-168.

Macdonald, F.A., Schmitz, M.D., Crowley, J.L., Roots, C.F., Jones, D.S., Maloof, A.C., Strauss, J.V., Cohen, P.A., Johnston, D.T., and Schrag, D.P. 2010, Calibrating the Cryogenian: Science, v. 327, p. 1241-1243.

Mattinson, J.M., 2005, Zircon U-Pb chemical abrasion ("CA-TIMS") method: Combined annealing and multi-step partial dissolution analysis for improved precision and accuracy of zircon ages: Chemical Geology, v. 220, p. 47-66.

Mattinson, J.M., 2010, Analysis of the relative decay constants of ^{235}U and ^{238}U by multi-step CA TIMS measurements of closed-system natural zircon samples: Chemical Geology, v. 275, p. 186-198.

McLean, N., Condon, D.J., Schoene, B., and Bowring, S.A., 2015, Evaluating Uncertainties in the Calibration of Isotopic Reference Materials and Multi-Element Isotopic Tracers (EARTHTIME Tracer Calibration Part II): Geochimica et Cosmochimica Acta, v. 164, p. 481-501.

Miller, R. McG., 2008, The Geology of Namibia: Neoproterozoic to lower Palaeozoic. Ministry of Mines and Energy, Geological Survey, Namibia.

Noble, S.R., Condon, D.J., Carney, J.N., Wilby, P.R., Pharoah, T.C., and Ford, T.D., 2015, U-Pb geochronology and global context of the Charnian Supergroup, UK: Constraints on age of key Ediacaran fossil assemblages. Geological Society of America Bulletin, v. 127, p. 250-265.

Och, L.M. & Shields-Zhou, G.A., 2012, The Neoproterozoic oxygenation event: Environmental perturbations and biogeochemical cycling: Earth-Science Reviews, v. 110, p. 26-57.

Rooney, A.D., Macdonald, F.A., Strauss, J.V., Dudás, F.Ö., Hallmann, C., and Selby, D., 2014, Re-Os geochronology and coupled Os-Sr isotope constraints on the Sturtian snowball Earth: Proceedings of the National Academy of Sciences, v. 111, p. 51-56.

Rooney, A.D., Strauss, J.V., Brandon, A.D., and Macdonald, F.A., 2015, A Cryogenian chronology: Two long-lasting synchronous Neoproterozoic glaciations: Geology, v. 43, p. 459-462.

Spence, G.H., Le Heron, D.P., and Fairchild, I.J., 2016, Sedimentological perspectives on climatic, atmospheric and environmental change in the Neoproterozoic Era: Sedimentology, v. 63, p. 253-306.

Sperling, E.A., Halverson, G.P., Knoll, A.H., Macdonald, F.A., and Johnston, D.T., 2013, A basin redox transect at the dawn of animal life: Earth and Planetary Science Letters, v. 371-372, p. 143-155.

Zhang, S., Jiang, G., and Han, Y. 2008, The age of the Nantuo Formation and Nantuo glaciation in South China: Terra Nova, v. 20, p. 289-294.

Zhou, C., Tucker, R, Xiao, S., Peng, Z. Yuan, X. and Chen, Z., 2004, New constraints on the ages of Neoproterozoic glaciations in south China: Geology, v. 32, p. 437-440.

Figure 1. Generalised geologic framework of northern Namibia. Ages for the Naauwpoort Formation (NF) and Oas Syenite (OS) are from Hoffman et al. (1996), for the Ombombo Subgroup from Halverson et al. (2005), and for the Ghaub Formation from Hoffmann et al. (2004) and this paper. See Miller (2008, and references therein) for the ages of the granites that post-date the Swakop Group rocks.

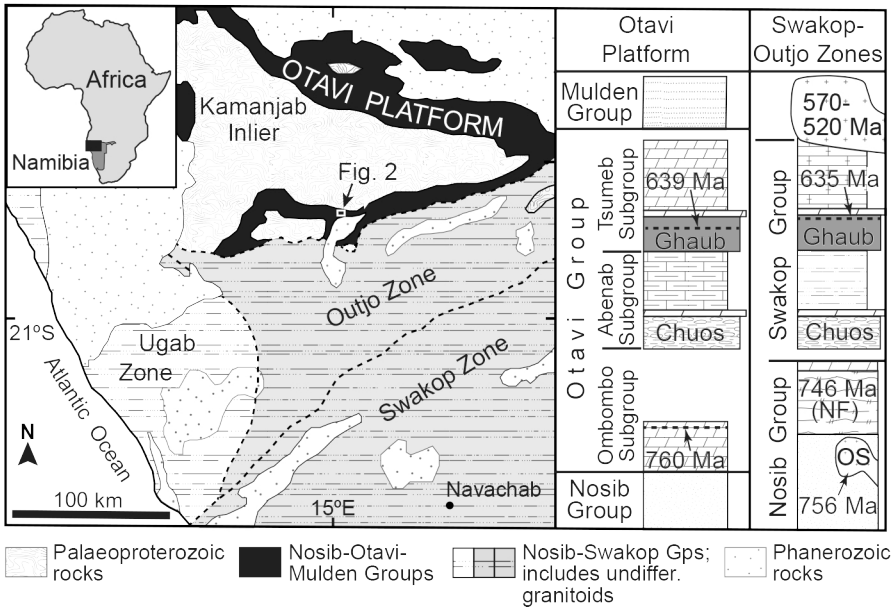

Figure 2. A. Fransfontein Ridge geology in the vicinity of sample DW-1. See Figure 1 for location.

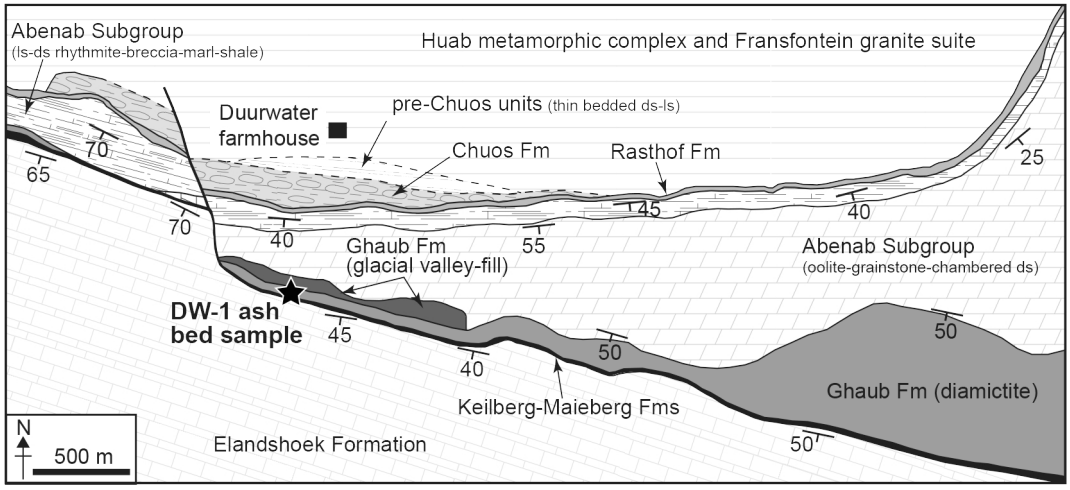

Figure 3. Simplified stratigraphy of the Duurwater and Navachab sections (for details of the Navachab section see Hoffmann et al., 2004); left column is a detailed section showing the stratigraphic position of the DW-1 ash bed within the diamictic interval of the Ghaub Formation.

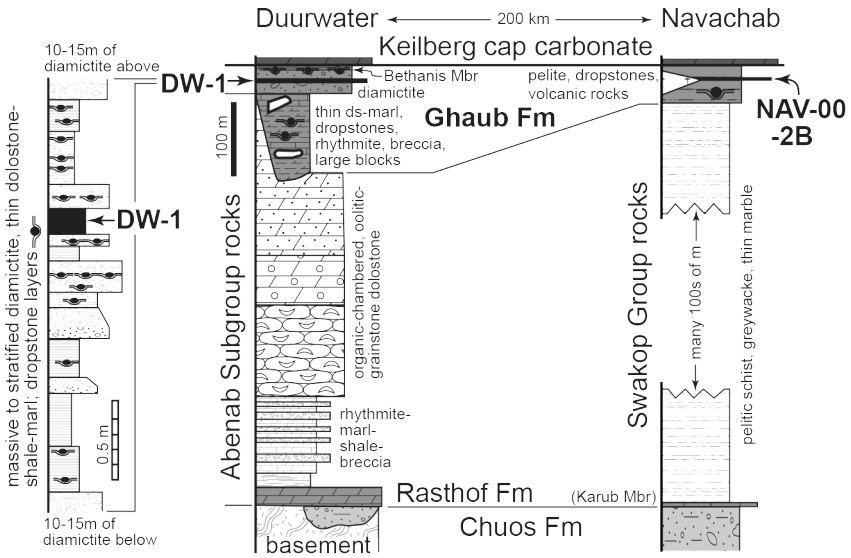

Figure 4. A. DW-1 ash bed between ice-rafted-debris beds, Duurwater section. **B.** U-Pb Concordia plot of data for samples DW-1 and NAV-00-2B; solid ellipses represent analyses included in age calculation, dashed ellipses are not included (see Data Repository for explanation). **C.** Neoproterozoic timeline trends for key isotope proxy datasets: S isotopes after (from Och and Shields-Zhou, 2012, and references therein); Sr and C isotopes after (Halverson et al., 2005) and our own data. U-Pb age data from: 1–Cox et al. (2015), 2–Macdonald et al. (2010), 3–Zhou et al. (2004), 4–Zhang et al. (2008), 5–Condon et al. (2005). Bold ages are reported herein.

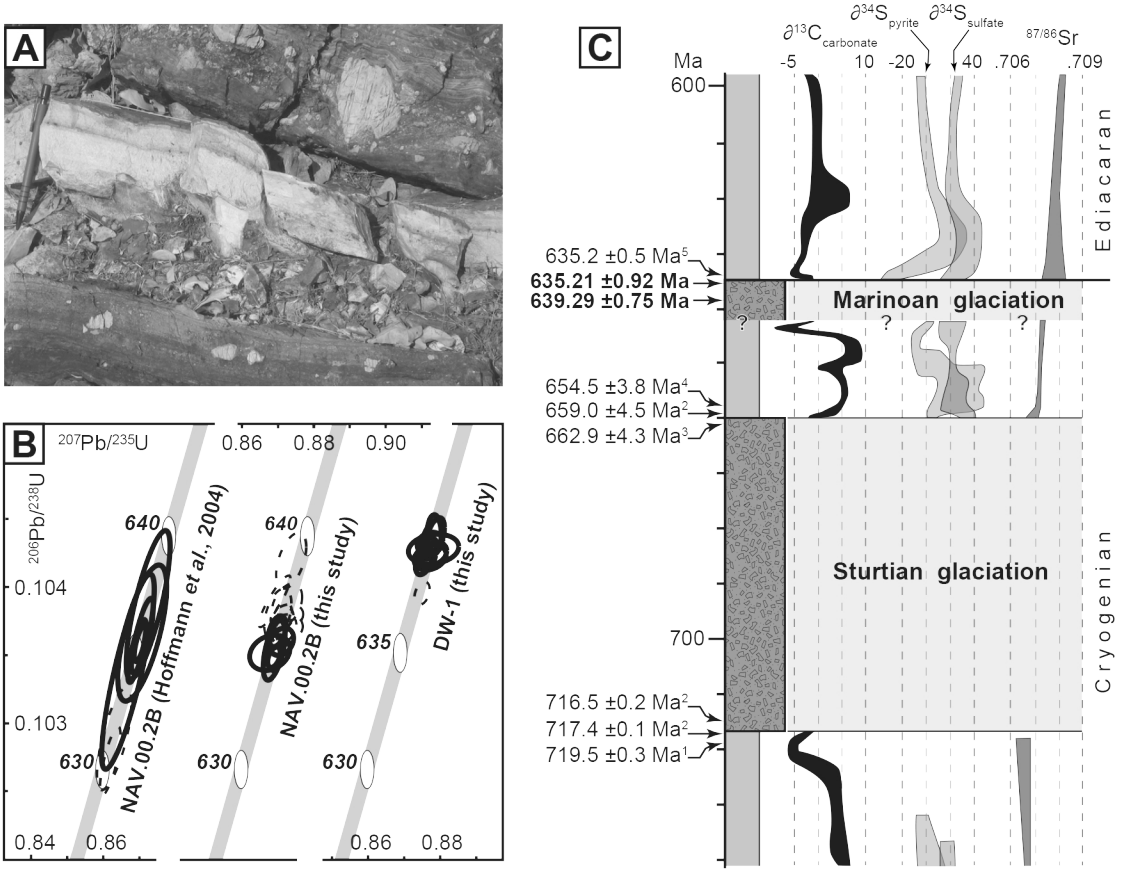

Supplementary File: Duration and nature of the end-Cryogenian (Marinoan) glaciation

[1]Anthony R. Prave, [2]Daniel J. Condon, [3]Karl Heinz Hoffmann, [2]Simon Tapster, and [4]Anthony E. Fallick

[1]Department of Earth and Environmental Science, University of St Andrews, St Andrews, KY16 9AL, United Kingdom
[2]NERC Isotope Geosciences Laboratory, British Geological Survey, Nottingham, NG12 5GG, United Kingdom
[3]Geological Survey of Namibia, 1 Aviation Road, Windhoek, Namibia
[4]Scottish Universities Environmental Research Centre, East Kilbride, G75 0QF, United Kingdom

U-Pb geochronology

U-Pb dates were obtained by the chemical abrasion isotope dilution thermal ionisation mass spectrometry (CA-ID-TIMS) method on selected single zircon grains (Tables 1 and 2), extracted from an aliquot of Sample DW-1 and NAV-00-2B. Sample DW-1 is located at 15.14693E 20.20940S; Sample NAV-00-2B was reported in Hoffmann et al. (2004).

Zircon grains were isolated from the rock sample using standard magnetic and density separation techniques, annealed in a muffle furnace at 900°C for 60 hours in quartz beakers. Zircon crystals, selected for analyses based on external morphology, were transferred to 3 ml Teflon PFA beakers, washed in dilute HNO_3 and water, and loaded into 300 µl Teflon PFA microcapsules. Fifteen microcapsules were placed in a large-capacity Parr vessel, and the crystals partially dissolved in 120 µl of 29 M HF for 12 hours at 180°C. The contents of each microcapsule were returned to 3 ml Teflon PFA beakers, the HF removed and the residual grains immersed in 3.5 M HNO3, ultrasonically cleaned for an hour, and fluxed on a hotplate at 80°C for an hour. The HNO_3 was removed and the grains were rinsed twice in ultrapure H_2O before being reloaded into the same 300 µl Teflon PFA microcapsules (rinsed and fluxed in 6 M HCl during crystal sonication and washing) and spiked with the EARTHTIME mixed ^{233}U-^{235}U-^{205}Pb-^{202}Pb tracer solution (ET2535). These chemically abraded grains were dissolved in Parr vessels in 120 µl of 29 M HF with a trace of 3.5 M HNO_3 at 220°C for 60 hours, dried to fluorides, and then re-dissolved in 6 M HCl at 180°C overnight. U and Pb were separated from the zircon matrix using an HCl-based anion exchange chromatographic procedure[1] eluted together and dried with 2 µl of 0.05N H_3PO_4.

Pb and U were loaded on a single outgassed Re filament in 5 µl of a silica-gel/phosphoric acid mixture[2], and U and Pb isotopic measurements made on a Thermo Triton multi-collector thermal ionisation mass spectrometer equipped with an ion-counting SEM detector. Pb isotopes were measured by peak-jumping all isotopes on the SEM detector for 100 to 150 cycles. Pb mass fractionation was externally corrected using a mass bias factor of 0.14 ± 0.03%/a.m.u. determined

via measurements of $^{202}Pb/^{205}Pb$ (ET2535)-spiked samples analysed during the same experimental period. Transitory isobaric interferences due to high-molecular weight organics, particularly on ^{204}Pb and ^{207}Pb, disappeared within approximately 30 cycles, and ionisation efficiency averaged 10^4 cps/pg of each Pb isotope. Linearity (to $\geq 1.4 \times 10^6$ cps) and the associated deadtime correction of the SEM detector were monitored by repeated analyses of NBS982, and have been constant since installation in 2006. Uranium was analysed as UO_2+ ions in static Faraday mode on 10^{12} ohm resistors for 150 to 200 cycles, and corrected for isobaric interference of $^{233}U^{18}O^{16}O$ on $^{235}U^{16}O^{16}O$ with an $^{18}O/^{16}O$ of 0.00206. Ionisation efficiency averaged 20 mV/ng of each U isotope. U mass fractionation was corrected using the known $^{233}U/^{235}U$ ratio of the ET2535 tracer solution.

Data reduction was done using the open-source ET Redux system[3,4] using the algorithms of McLean et al.[4], ET2535 tracer solution[5,6] and U decay constants recommended by Jaffey et al.[7]. A value of 138.818 ± 0.045 was used for the $^{238}U/^{235}U_{zircon}$ based upon the work of[8] whereas a value of 137.88 was used in the prior study[20] study. $^{206}Pb/^{238}U$ ratios and dates were corrected for initial ^{230}Th disequilibrium using a Th/U[magma] = 3 ±1 resulting in an increase in the $^{206}Pb/^{238}U$ dates of ~0.09 Myr (no Th correction was made for date presented in Hoffmann et al.[9]. All common Pb in analyses was attributed to laboratory blank and subtracted based on the measured laboratory Pb isotopic composition and associated uncertainty. U blanks were estimated at 0.1 pg, based upon replicate total procedural blanks.

In this manuscript the date uncertainties reporting is as A/B/C and reflect the following sources: (A) analytical, (B) analytical + tracer solution and (C) analytical + tracer solution + decay constants. The A uncertainty is the internal error based on analytical uncertainties only, including counting statistics, subtraction of tracer solution, and blank and initial common Pb subtraction. It is given at the 2σ confidence interval. This error should be considered when comparing our date with $^{206}Pb/^{238}U$ dates from other laboratories that used the same EARTHTIME tracer solution or a tracer solution that was cross-calibrated using related gravimetric reference materials. The B uncertainty includes uncertainty in the tracer calibration and should be used when comparing our dates with those derived from laboratories that did not use the same EARTHTIME tracer solution or a tracer solution that was cross-calibrated using relatable gravimetric reference material[9,10]. The C uncertainty includes A and B in addition to uncertainty in the ^{238}U decay constant[7]. This uncertainty level should be used when comparing our dates with those derived from other decay schemes (e.g. $^{40}Ar/^{39}Ar$, ^{187}Re-^{187}Os).

Ten zircon U-Pb dates were obtained and are presented in Supplementary Table 1 (and Figure 6A of the main paper). All dates are concordant and yield a weighted mean $^{207}Pb/^{206}Pb$ date of 639.1 ± 1.7/1.8/5.0 Ma (MSWD = 0.38, n = 10). The U-Pb data for this same sample dataset is not so simple and does not form a coherent population and yield an MSWD that indicates excess scatter. One fraction (z16) is distinctly younger than the main cluster (see Fig. 6A main paper) and is considered to reflect residual Pb-loss. The remaining nine data points yield a weighted mean $^{206}Pb/^{238}U$ date of 639.59±0.42 Ma (internal uncertainties only 95% conf., MSWD = 6.4), but with an MSWD value that still indicates excess scatter. Evaluation of this dataset shows a strong clustering around 639.5 Ma and yield a weighted mean $^{206}Pb/^{238}U$ date of 639.29 ± 0.26/0.31/0.75 Ma (95% conf. MSWD = 2.6). We consider this to be the best approximation of the zircon population within sample DW-1 that best represents the timing of eruption, and hence the age for the stratigraphic level at which DW-1 was sampled within the Ghaub Formation.

Fifteen zircon U-Pb dates are presented in Table 1 and are presented graphically in Figure 6A of the main paper. A coherent set of $^{207}Pb/^{206}Pb$ dates yield a weighted mean $^{207}Pb/^{206}Pb$ date of 634.8 ± 1.5/1.7/4.9 Ma (MSWD = 0.96, n = 15). The U-Pb data for this same sample dataset is also not so simple and does not form a coherent population. One fraction (z12) is normally discordant with a younger U-Pb age indicating Pb-loss and is disregarded from further discussion. The remaining fractions have $^{238}U/^{206}Pb$ dates that do not overlap and there is no correlation with $^{207}Pb/^{238}U$ dates such that the data form a short linear array that plots across the concordia band (defined by the ^{235}U and ^{238}U decay constants uncertainties[7]), with two values reversely discordant. Based upon analyses of chemically abraded zircon data we would expect closed system zircon to plot towards the lower limits of the concordia uncertainty band[11,12]. However, in this data set, analyses plot from this region towards and across the upper uncertainty bound (see Fig. 6A in the main paper). Based upon long-term reproducibility of U-Pb data from the NIGL ID-TIMS laboratory, and coherent U-Pb data obtained for a high proportion of samples analysed, we suggest this variation is real and not an artefact of mass spectrometry and that this reflects real U/Pb variation in the analysed sample (which has been annealed and leached). One option is that the older U-Pb dates reflecting analyses of pre-eruptive zircon, and the apparent lack of corresponding variation in the $^{207}Pb/^{206}Pb$ dates is due to being obscured by their larger uncertainties. An alternative is that the analyses with older $^{238}U/^{206}Pb$ dates are from a single concordant age population and that these older dates reflect un-supported radiogenic Pb. Whilst this is unlikely to occur at a bulk level (i.e., single crystal) it is possible that in zircons with fine scale U zonation redistribution of radiogenic Pb occurs at the sub-micron level[13,14], which is then enhanced by the thermal annealing and chemical leaching process[15]. This possibility requires further investigation.

Either of these scenarios for explaining the scatter in the NAV-00-2B U-Pb require an interpretive framework where the younger dates are considered to most closely reflect the age of the erupted zircons and inferentially the age of the ash layer. This in turn requires the subjective selection of a date from which to derive an interpreted age for the sample. In Figure 1 we show a number of viable interpretations for this sample, selecting different sub-populations from the cluster of youngest dates. Our preferred interpreted date is Interpretation B, a weighted mean $^{206}Pb/^{238}U$ date based upon the youngest five dates: 635.21 ± 0.59/0.61/0.92 Ma (95% conf. MSWD = 3.4). We consider this to be the best approximation of the zircon population within sample NAV-00-2B that best represents the timing of eruption, and hence the age for the stratigraphic level at which NAV-00-2B was sampled within the Ghaub Formation. Each of the other alternative interpreted ages (Fig. 1) overlap with each other and thus the choice of interpreted date has no significant impact. We consider that alternative interpretations based upon the older age (ca. 636.5 Ma) are much more difficult to justify as they require the cluster of concordant overlapping dates at ca. 635.5 Ma to be too young due to Pb-loss, which we consider highly unlikely.

References cited

1. Krogh, T. E., 1973, A low contamination method for hydrothermal decomposition of zircon and extraction of U and Pb for isotopic age determination. *Geochimica et Cosmochimica Acta* 37, 485-494.
2. Gerstenberger, H. and Haase, G., 1977, A highly effective emitter substance for mass spectrometric Pb isotope ratio determinations. *Chemical Geology* 136, 309.
3. Bowring, J. F., McLean, N. M., and Bowring, S. A., 2011, Engineering cyber infrastructure for U-Pb geochronology: Tripoli and U-Pb_Redux. *Geochem. Geophys. Geosyst.* 12, Q0AA19, doi:10.1029/2010gc003479.
4. McLean, N., Bowring, J., and Bowring, S., 2011, An Algorithm for U-Pb Isotope Dilution Data Reduction and Uncertainty Propagation. *Geochemistry Geophysics Geosystems*.
5. McLean, N., Condon, D. J., Schoene, B., and Bowring, S. A., 2015, Evaluating Uncertainties in the Calibration of Isotopic Reference Materials and Multi-Element Isotopic Tracers (EARTHTIME Tracer Calibration Part II). *Geochimica et Cosmochimica Acta*, doi:10.1016/j.gca.2015.02.040.
6. Condon, D. J., Schoene, B., Mclean, N., Bowring, S. A., and Parrish, R., 2015, Metrology and Traceability of U-Pb Isotope Dilution Geochronology (EARTHTIME Tracer Calibration Part I). *Geochimica et Cosmochimica Acta*, doi:10.1016/j.gca.2015.05.026.

142 7. Jaffey, A. H., Flynn, K. F., Glendenin, L. E., Bentley, W. C., and Essling, A. M., 1971, Precision
143 measurement of half-lives and specific of ^{235}U and ^{238}U. *Physics Reviews* C4, 1889-1906.
144 8. Hiess, J., Condon, D. J., McLean, N., and Noble, S. R., 2012, $^{238}U/^{235}U$ Systematics in Terrestrial
145 Uranium-Bearing Minerals. *Science* 335, 1610-1614, doi:10.1126/science.1215507.
146 9. Hoffmann, K.-H., Condon, D., Bowring, S., and Crowley, J., 2004, U-Pb zircon date from the
147 Neoproterozoic Ghaub Formation, Namibia: constraints on Marinoan glaciation. *Geology*
148 32, 817.
149 10. Condon, D. *et al.*, 2005, U-Pb ages from the Neoproterozoic Doushantuo formation, China.
150 *Science* 308, 95.
151 11. Mattinson, J. M., 2010, Analysis of the relative decay constants of 235U and 238U by multi-
152 step CA-TIMS measurements of closed-system natural zircon samples. *Chemical Geology*
153 275, 186-198.
154 12. Schoene, B., Crowley, J. L., Condon, D. J., Schmitz, M. D., and Bowring, S. A., 2006,
155 Reassessing the uranium decay constants for geochronology using ID-TIMS U-Pb data.
156 *Geochimica et Cosmochimica Acta* 70, 426-445.
157 13. Mattinson, J. M., Graubard, C. M., Parkinson, D. L., and McClelland, W. C., 1996, in *Earth*
158 *Processes: Reading the Isotopic Code* 355-370. American Geophysical Union.
159 14. Williams, I. S., Compston, W., Black, L. P., Ireland, T. R., and Foster, J. J., 1984, Unsupported
160 radiogenic Pb in zircon: a cause of anomalously high Pb-Pb, U-Pb and Th-Pb ages. *Contrib*
161 *Mineral Petrol* 88, 322-327, doi:10.1007/BF00376756.
162 15. Mattinson, J. M., 2005, Zircon U-Pb chemical abrasion ("CA-TIMS") method: Combined
163 annealing and multi-step partial dissolution analysis for improved precision and accuracy of
164 zircon ages. *Chemical Geology* 220, 47-66.
165
166

Supplementary File Table 1. U-Pb analyses of Sample DW-1.

Table 1. U-Pb geochronology data for Sample DW-1

DW-1

Fraction	Dates (Ma) 206Pb/ 238U a	±2σ abs	207Pb/ 235U a	±2σ abs	207Pb/ 206Pb a	±2σ abs	Corr. coef.	% disc b	Composition Th/ U c	Pb* (pg) d	Pbc (pg) e	Pb*/ Pbc f
Zircon												
z4	639.8913333	0.593356873			3143716	5.254532308	0.46132761	-0.090246937	0.327013873	11.0945386	0.319776778	34.69463498
z11	639.9597341	0.61116763			0903181	4.419005959	0.444784829	0.176353311	0.333060166	38.57476318	1.064909851	36.22350112
z16	637.4957221	0.40515678			6570565	3.932135184	0.35297439	0.493451899	0.32174235	19.93618539	0.43823687	45.49180309
z17	639.0061232	0.303639676			0301121	5.005617457	0.249856013	-0.152972577	0.323888831	30.22943263	0.902513177	33.49472718
z21	638.8758748	0.477552232	638.4905503	1.058814803	637.1271885	4.310621783	0.454308748	-0.274464237	0.30921582	13.59503911	0.288702932	47.09006243
z22	639.6185865	0.385317862	639.3808723	1.567990007	638.5409702	6.992279451	0.18125451	-0.168762282	0.323381833	12.20140233	0.5066661	24.08174208
z24	639.3983143	0.357451224	639.2112335	0.995533127	638.5500308	4.275124401	0.324633254	-0.132845268	0.303400454	12.45031276	0.298627603	41.69176809
z25	639.0243525	0.437395676	639.3931888	1.951032642	640.6967066	8.618269804	0.231042999	0.26102117	0.317045465	13.53249896	0.744581906	18.17462772
z26	639.1746318	0.395637107	639.8462088	1.663527279	642.2181997	7.280926619	0.270989422	0.473914918	0.322849444	9.54954437	0.394464528	24.20887988
z27	639.3743696	0.518935497	639.9054507	3.063162745	641.7809117	13.69295819	0.163923419	0.374978758	0.322526696	18.45161327	1.643269872	11.22859585

Mean = 639.29±0.26 [0.041%] 95% conf.
Wtd by data-pt errs only, 0 of 9 rej.
MSWD = 2.6, probability = 0.008

Fraction	Isotopic Ratios 206Pb/ 204Pb g	206Pb/ 238U h	±2σ %	207Pb/ 235U h	±2σ %	207Pb/ 206Pb h	±2σ %	208Pb/ 232Th h	±2σ %
z4	2191.901766	0.104356865	0.097406106	0.877744978	0.273430886	0.0610295	0.242138987	-	-
z11	2283.914697	0.104368583	0.100319739	0.878568751	0.229445772	0.061079918	0.202943566	-	-
z16	2872.317701	0.103946541	0.066748714	0.874839743	0.195417113	0.061067613	0.179965816	-	-
z17	2118.54203	0.104205227	0.049911498	0.875946448	0.240065945	0.060993075	0.23040829	-	-
z21	2982.862756	0.104182917	0.078514014	0.875391464	0.223398226	0.060967484	0.197704085	-	-
z22	1528.448508	0.104310141	0.063279853	0.877036592	0.330497673	0.061007561	0.323425933	-	-
z24	2647.031	0.104272408	0.058722617	0.876723024	0.209876385	0.061007818	0.19607984	-	-
z25	1159.850691	0.10420835	0.07189601	0.87705936	0.411228915	0.061068739	0.399461002	-	-
z26	1536.499467	0.104234091	0.065017487	0.877897009	0.350451737	0.061111967	0.337115973	-	-
z27	722.4353758	0.104268306	0.08525453	0.878006577	0.645267067	0.061099539	0.636046517	-	-

a Isotopic dates calculated using the decay constants λ238 = 1.55125E-10 and λ235 = 9.8485E-10 (Jaffey et al. 1971).
b % discordance = 100 - (100 * (206Pb/238U date) / (207Pb/206Pb date))
c Th contents calculated from radiogenic 208Pb and the 230Th-corrected 206Pb/238U date of the sample, assuming concordance between the U-Pb and Th-Pb systems.
d Total mass of radiogenic Pb.
e Total mass of common Pb.
f Ratio of radiogenic Pb (including 208Pb) to common Pb.
g Measured ratio corrected for fractionation and spike contribution only.
h Measured ratios corrected for fractionation, tracer and blank.

Supplementary File Table 2. U-Pb analyses of Sample NAV-00-2B.

Table 2. U-Pb geochronology data table for Sample NAV-00-2B

NAV-00-2B

Fraction	Dates (Ma) 206Pb/ 238U a	±2σ abs	207Pb/ 235U a	±2σ abs	207Pb/ 206Pb a	±2σ abs	Corr. coef.	% disc b	Composition Th/ U c	Pb* (pg) d	Pbc (pg) e	Pb*/ Pbc f
Zircon												
~~z1~~	~~630.325841~~	~~1.427257764~~	~~632.3425419~~	~~1.500599293~~	~~639.5593176~~	~~4.16779408~~	~~0.795684556~~	~~1.443724817~~	~~0.98958822~~	~~25.95531637~~	~~0.244748012~~	~~106.0491409~~
z2	**634.8152933**	**0.361089668**			229458	3.268830557	0.442587284	0.111349646	0.781902518	32.11375832	0.488536297	65.73464149
z3	**635.0074513**	**0.616782193**			642267	11.02132127	0.224344287	-0.481550138	0.836137413	29.01789356	1.796549443	16.152015
z4	**635.1102299**	**1.041523352**			918621	5.189286138	0.552189166	-0.081685227	0.914774793	9.246059087	0.185963632	49.71971655
z5	**635.4811482**	**0.480901223**			428952	6.55450615	0.261349317	0.44830873	0.921515449	24.2462356	0.818413401	29.62590246
z6	**635.9269141**	**0.537359089**			7631766	4.551318296	0.3880762	-0.34141104	0.689124473	17.39778845	0.399523434	43.54635294
z7	636.0251646	0.491656154	636.4320058	1.569225339	637.8769387	6.814527199	0.304270314	0.290302723	0.793830482	20.44741294	0.770848267	26.52585963
z8	636.0837863	0.465091109	636.9009847	1.969787668	639.8016166	8.951018375	0.094388782	0.58109111	0.688131315	21.51517978	1.116393504	19.27203956
z9	636.4896941	0.346890026	636.6197383	1.05222859	637.0814001	4.612233493	0.268022026	0.092877607	0.89792076	25.57007839	0.56140369	45.54668745
z10	636.5327889	0.450326407	636.9122513	2.014466507	638.2588544	8.926365678	0.231526821	0.270433457	1.003725792	29.83487454	1.432269794	20.83048505
z11	636.5415143	0.530421956	636.3381731	1.125291111	635.6160755	5.042806223	0.225758259	-0.145597133	0.99329867	14.90304587	0.203369322	73.28069793
z12	636.6413477	0.907141109	635.5496194	1.665459327	631.6691892	6.851032134	0.431192877	-0.787145967	0.688643899	8.542737957	0.259901246	32.86916894
z13	637.0590132	0.742630458	636.914865	1.878832927	636.4034476	7.940933599	0.375616243	-0.103011012	0.889628354	27.29746509	0.783902052	34.8225458
z14	637.2110942	0.904405834	635.060404	1.952228537	627.413444	6.212033955	0.893290154	-1.56159392	0.927082525	11.04128128	0.315825711	34.96004566
z15	638.9526717	0.97786515	637.5635782	1.842922873	632.6433353	7.314631558	0.495113811	-0.997297539	1.018274826	9.36347568	0.244435542	38.30652286

Mean = 635.48±0.53 [0.083%] 95% conf.
Wtd by data-pt errs only, 0 of 7 rej.
MSWD = 5.1, probability = 0.000

Fraction	Isotopic Ratios 206Pb/ 204Pb g	206Pb/ 238U h	±2σ %	207Pb/ 235U h	±2σ %	207Pb/ 206Pb h	±2σ %	208Pb/ 232Th h	±2σ %
~~z1~~	~~5657.914072~~	~~0.102719384~~	~~0.237682284~~	~~0.864070528~~	~~0.318821774~~	~~0.06103645~~	~~0.191054195~~	—	—
z2	3688.313952	0.103487614	0.059727721	0.868901235	0.168555117	0.060922052	0.148389858	-	-
z3	908.4355099	0.103520508	0.101992359	0.867741875	0.524910654	0.060821432	0.510749441	-	-
z4	2708.596134	0.103538102	0.1722019	0.868949178	0.288743899	0.060895704	0.238887211	-	-
z5	1618.630386	0.1036016	0.079466399	0.870998998	0.315635823	0.061001944	0.302957196	-	-
z6	2504.826885	0.103677916	0.088736539	0.869787694	0.229380104	0.060872268	0.20891154	-	-
z7	1494.863496	0.103694737	0.081177473	0.871593226	0.331858556	0.060988733	0.315085512	-	-
z8	1118.756286	0.103704774	0.076784578	0.872457866	0.416348587	0.061043327	0.414921316	-	-
z9	2492.366572	0.103774273	0.057235328	0.871939294	0.222477296	0.060966187	0.211893889	-	-
z10	1122.441766	0.103781652	0.07429709	0.872478643	0.425786815	0.060999561	0.413664883	-	-
z11	3912.570586	0.103783146	0.08751051	0.871420278	0.238000926	0.060924688	0.232058769	-	-
z12	1895.423855	0.10380024	0.149640369	0.869967484	0.352561718	0.060813101	0.316460832	-	-
z13	1913.492038	0.103871757	0.122426573	0.872483463	0.397117512	0.060946982	0.367586862	-	-
z14	1904.844159	0.1038978	0.149062248	0.869066744	0.413497059	0.060693092	0.286414064	-	-
z15	2042.545659	0.104196072	0.160751715	0.873680147	0.389242486	0.060840616	0.338147365	-	-

a Isotopic dates calculated using the decay constants λ238 = 1.55125E-10 and λ235 = 9.8485E-10 (Jaffey et al. 1971).
b % discordance = 100 - (100 * (206Pb/238U date) / (207Pb/206Pb date))
c Th contents calculated from radiogenic 208Pb and the 230Th-corrected 206Pb/238U date of the sample, assuming concordance between the U-Pb and Th-Pb systems.
d Total mass of radiogenic Pb.
e Total mass of common Pb.
f Ratio of radiogenic Pb (including 208Pb) to common Pb.
g Measured ratio corrected for fractionation and spike contribution only.
h Measured ratios corrected for fractionation, tracer and blank.

Supplementary File Figure 1. U-Pb concordia diagram for zircon analyses of Sample NAV-00-2B.